 doi:10.20944/preprints202101.0593.v1

Article

Electrodeposition of Copper and Brass Coatings with Olive-like Structure

Artur Maciej [1,*], Natalia Łatanik [1], Maciej Sowa [1] and Wojciech Simka [1]

[1] Silesian University of Technology, Faculty of Chemistry, B. Krzywoustego Str. 6, 44-100 Gliwice, Poland; RCh1@polsl.pl
* Correspondence: artur.maciej@polsl.pl

Abstract: One method of creating a brass coating is through electrodeposition, which is most often completed in cyanide galvanic baths. Because of the toxicity of cyanides, many are working on the development of cyanide-free baths, which are promising but not satisfactory to replace the classic methods. The purpose of the study was to explore a new generation of non-aqueous cyanide-free baths based on 1-ethyl-3-methylimidazolium acetate ionic liquids. The study involved the formation of copper, zinc, and brass coatings. The influence of the bath composition, cathodic current density, and temperature was determined. The obtained coatings were characterized by their morphology, chemical composition, roughness, and corrosion resistance. It was found that the structure of the obtained coatings is strongly dependent on the process parameters. The three main structures observed were fine-grained, porous, and olive-like. To the best knowledge of the authors, it is the first time the olive-like structure was observed in the case of an electrodeposited coating. The Cu-Zn coatings consisted of 19–96 at.% copper and exhibited relatively strong corrosion resistance. High improvement of corrosion properties was found in the case of copper and brass coatings with an olive-like structure.

Keywords: brass coating; Cu-Zn alloy coating; electrodeposition; non-cyanide bath; ionic liquids; 1-ethyl-3-methylimidazolium acetate; olive-like structure

Citation: Maciej, A.; Łatanik, N.; Sowa, M.; Simka, W. Electrodeposition of brass coatings of olive-like structure. *Materials* **2021**, *14*, x. https://doi.org/10.3390/xxxxx

1. Introduction

The most popular method to create alloys is based on melting and molding the components of the alloy; however, it is not the only technique used to produce alloys. Alloys may also be formed by other methods, e.g., sintering of metallic powders [1], diffusion saturation [2], and ion implantation [3]. Because of the high energy consumption, these methods are relatively costly, so they are only used in some specific cases where the conventional method is not economically justified, e.g., formation of alloys of refractory metals (W, Mo, Ta). Moreover, alloys may also be formed during the process of electrodeposition, which is particularly interesting if the alloy is used as a coating. Electrodeposition of alloy coatings has many advantages, which are not present in the coatings obtained by other methods. First, the process is completed at a relatively low temperature (up to several dozen of °C), avoiding high costs of heating and melting the metals. The chemical composition as well as the structure of the electrodeposited alloys may be easily modified by galvanic bath composition or process parameters (e.g., current density). The method allows the formation of some phases which are impossible or hard to obtain by metallurgical methods. The thickness of the electrodeposited coatings is also uniform and easy to adjust. Moreover, the alloys obtained by electrodeposition are characterized by lower porosities relative to casted alloys or alloys formed by sintering of metallic powders [4]. The

Preprints (www.preprints.org) | NOT PEER-REVIEWED | Posted: 28 January 2021 doi:10.20944/preprints202101.0593.v1

most popular and effective method of copper-zinc alloy (brass) coating formation is electrodeposition in a cyanide solution. The galvanic baths have a high throwing power, the quality of the coatings is very good, and the current efficiency of the process is relatively high. Despite the high toxicity of cyanides and the strict maintenance control, the baths have been widely used in the production of brass alloy coatings [5]. There are many reports describing a possibility of electrodeposition of Cu-Zn alloys in cyanide-free baths, e.g., pyrophosphate [6,7], citrate [8], oxalate [9], tartrate [10], EDTA [11], triethanolamine [12], ammonia [13], glucoheptonate [14], glutamate [15] and glycinate [16] baths. The electrodeposited brass may be used as a matrix in the brass-composite coatings. These materials have been found to have improved properties such as an increase in the tribological properties in the case of graphite – brass coating [17] and improved scratch and corrosion resistance in the case of Cu_5Zn_8 – brass intermetallic composite coating [18].

A new generation group of galvanic baths based on deep eutectic solvents (DESs) or ionic liquids (ILs) has been developed. Most often, these methods have many advantages such as being considered green solvents as well as typically having low vapor pressures, non-flammability, high thermal stability, and a wide electrochemical window [19,20]. The most popular DESs used in electrodeposition are based on choline salt mixtures [21], mainly with urea [22], thiourea [23], ethylene glycol [24] or salts being the source of the deposited metals [25]. Any one of these options may be successfully used as a cyanide-free galvanic bath for Cu-Zn alloy coatings. Xie et al. [26] investigated the electrodeposition of Zn and Cu-Zn coatings from a choline chloride/urea-based DES with ZnO and CuO precursors. The conditions for uniform, dense, and compact coatings were determined. Moreover, it was found that the compact, flat, and fine particles ensured improved corrosion resistance in a sodium chloride solution. Electrodeposition of brass coatings was also investigated by Fricoteaux et al. [27] using a 1-butyl-1-methylpyrrolidinium bis(trifluoromethylsulfonyl)imide IL. The authors reported that the electrodeposition of Zn, Cu and Cu-Zn coatings is possible from ILs without the use of chloride anions. The obtained deposits had different morphologies and phase compositions corresponding to the mixtures of different Cu-Zn phases that were obtained from a range of applied potentials. It was found that between a specific range of potentials (from –1.6V/Ag to 2.25V/Ag), the zinc content in the alloy decreased and the coatings became amorphous. Zhang et al. [28] also studied the Cu-Zn electrodeposition coating process when using 1-ethyl-3-methylimidazolium trifluoromethylsulfonate IL and ethanol mixtures to replace the highly-poisonous cyanide zincate process. The Zn content in the obtained coatings was up to 30 at.%. It was reported that under optimal conditions, the cauliflower-shaped Cu_5Zn_8 alloy displayed a significant improvement in corrosion resistance when electrodeposited. The authors of this paper have considered using galvanic baths based on 1-ethyl-3-methylimidazolium acetate ([EMIM][Ac]) IL to eliminate the use of cyanide in aqueous baths for the electrodeposition of brass coatings.

2. Materials and Methods

2.1. ElectrodepositionElectrodeposition of Zn, Cu and Cu-Zn coatings on steel

Copper, zinc and Cu-Zn alloy coatings were electrodeposited on a S235JR carbon steel substrate (Table 1) in baths composed of 1-ethyl-3-methylimidazolium acetate ([EMIM][Ac]) and acetate(s) of appropriate metal(s), i.e., copper acetate (CuAc: 5–80 mg/mL) for copper electrodeposition, zinc acetate (ZnAc: 5–800 mg/mL) for zinc electrodeposition or both of the salts (CuAc and ZnAc) for the brass coatings.

Table 1. Chemical composition of S235JR carbon steel (wt. %).

C	Mn	Si	P	S	Cr	Ni	Cu	Al	Fe
≤ 0.22	≤ 1.1	≤ 0.35	≤ 0.05	≤ 0.05	≤ 0.30	≤ 0.30	≤ 0.30	0.02	remain

Preprints (www.preprints.org) | NOT PEER-REVIEWED | Posted: 28 January 2021 doi:10.20944/preprints202101.0593.v1

The electrodeposition of copper and zinc was conducted at a cathodic current density (jc) of 0.75–48.0 mA/cm2 and at a temperature of 25; 50; 75 and 100°C. The steel samples were used as the cathode (substrate), and platinum plates were used as anodes.

The parameters of the Cu-Zn electrodeposition coatings were selected based on the studies of copper and zinc formation in the acetate baths. Four galvanic baths based on 1-ethyl-3-methylimidazolium acetate were prepared for the investigation; their composition is presented in Table 2. The process was conducted in the promising range of cathodic current density (1.5; 3; 6 and 12 mA·cm-2) and at favorable temperature (100°C).

Table 2. Chemical composition of the galvanic baths for Cu-Zn coatings electrodeposition

Component	CuZn-1 bath	CuZn-2 bath	CuZn-3 bath	CuZn-4 bath
EMIM[Ac]	Basic electrolyte (solvent)			
CuAc	60 mg/mL	60 mg/mL	60 mg/mL	60 mg/mL
ZnAc	480 mg/mL	600 mg/mL	800 mg/mL	1000 mg/mL

2.2. Characterization

The surface morphology was investigated by a Phenom ProX (Thermo Fisher Scientific, USA) scanning electron microscope (SEM) equipped with an energy dispersive X-ray spectroscopy (EDX) analyzer to determine the chemical composition. The roughness of the coatings was determined based on 3D surface reconstructions obtained by the SEM and served to generate microroughness profiles of the coatings. The profiles were used to calculate the arithmetic roughness coefficient (Ra) and the maximum height of the profile (Rz). The chemical compositions of the brass coatings were also analyzed by inductively coupled plasma optical emission spectroscopy (ICP-OES) by an ICP-OES Varian 710-ES spectrometer (Varian Inc., USA) after digestion of the coatings in 10% HNO_3 at a temperature of 60°C. The corrosion resistance studies of the electrodeposited coatings were completed by the potentiodynamic Tafel method using an AUTOLAB PGSTAT100 (Metrohm) potentiostat-galvanostat. The corrosion measurements were carried out in a 5% solution of NaCl at a temperature of 25°C. The samples were stabilized at open circuit (up to 1 h) before the polarization and open circuit potentials (E_{OC}) were determined. The potentiodynamic measurements (linear sweep voltammetry – LSV) were carried at potentials between E_{OC} –150 mV and E_{OC} +150 mV with a scan rate of 0.1 mV·s^{-1}. The obtained voltammograms were analyzed by NOVA 2.1. software, which was able to obtain corrosion properties of resistance polarization (R_p), corrosion current density (j_{corr}), and corrosion potential (E_{corr}). A double-walled (thermostatic) electrochemical cell with a three-electrode configuration was used. A saturated calomel electrode (SCE) served as the reference electrode, and a platinum mesh served as the counter electrode.

3. Results and Discussion

3.1. Surface morphology – SEM analysis

3.1.1. Copper coatings

The effect of copper acetate concentration, temperature, and cathodic current density on the structure of the copper coatings was investigated. All parameters had an influence on the likelihood of the coating forming and each coating's morphology. In the baths with low concentrations of copper salts (5–10 mg/mL), the electrodeposition of the coating was not possible. Electrodeposition of copper is only feasible in baths with relatively high concentrations of the metal, especially at elevated temperatures (75°C, 100°C). Small amounts of copper in the form of islands were electrodeposited from the baths with a relatively low concentration of copper acetate: 20–30 mg/mL (Figure 1). The observed type of crystallization occurred through Volmer-Weber island growth, which resulted from the diffusion-limited regimes [29].

Preprints (www.preprints.org) | NOT PEER-REVIEWED | Posted: 28 January 2021 doi:10.20944/preprints202101.0593.v1

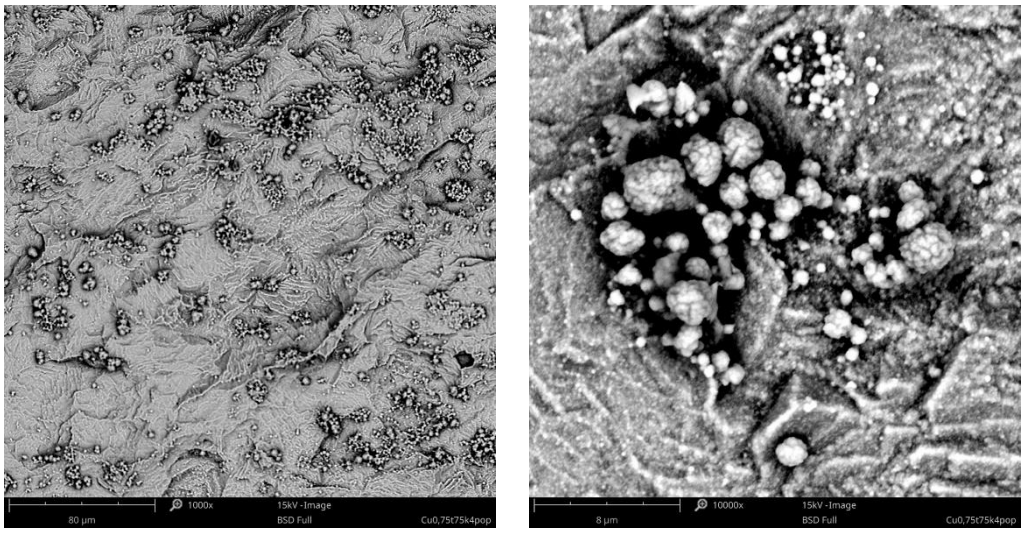

(**a**) (**b**)

Figure 1. SEM images of Cu island electrodeposited in the bath with 20 mg/mL of CuAc at a temperature of 75°C (j_c = 0.75 mA·cm^{-2}, t = 1h); Magnification: (**a**) x1000; (**b**) x 10000.

Some of the obtained coatings had very characteristic, porous structures, which is not typical for electrodeposited coatings. Specific process parameters led to these structures. It was observed that the homogeneous, porous coatings with pores sizes less than 500 nm were obtained in a bath with 30 g/dm^3 of CuAc at a temperature of 75°C (Figure 2a). Other porous coatings were obtained in a bath containing 35 mg/mL of CuAc at a temperature of 25°C (Figure 2b).

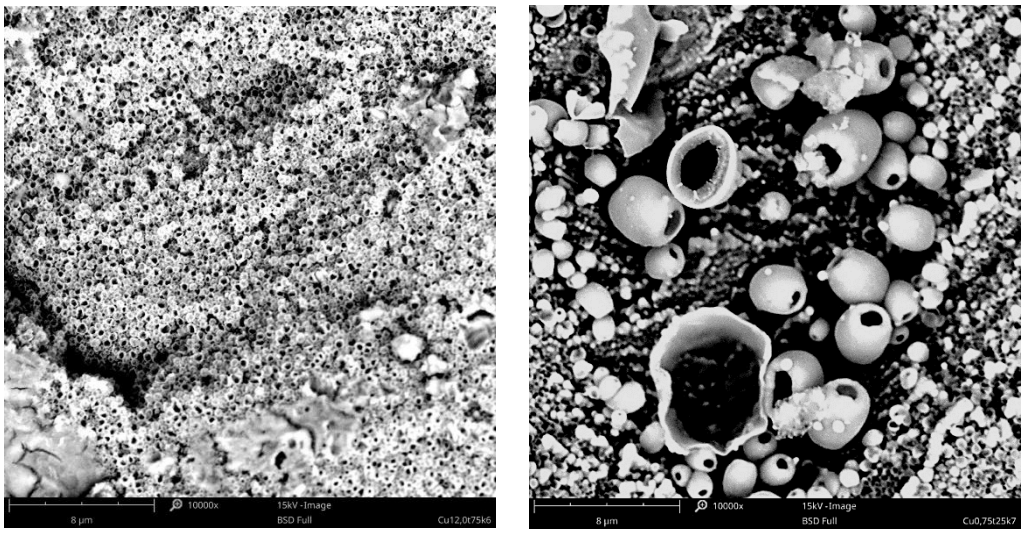

(**a**) (**b**)

Figure 2. SEM images of the porous Cu coating electrodeposited in the bath with:
a) 30 mg/mL of CuAc (T = 75°C, j_c = 12 mA·cm^{-2}, t = 7.5 min), magn.: x10000;
b) 35 mg/mL of CuAc (T = 25°C, j_c = 0,75 mA/cm^{-2}, t = 1 h), magn.: x10000.

To the best knowledge of the authors, it is the first time that the olive-like structure was observed in an electrodeposited coating. A similar structure has been seen by Rokosz et al. [30,31] and Komarova et al. [32] in the case of oxide coatings obtained by a plasma electrolytic oxidation (PEO) process of titanium, but the mechanism by which the structure forms is drastically different. The most probable mechanism of the olive-like struc-

Preprints (www.preprints.org) | NOT PEER-REVIEWED | Posted: 28 January 2021 doi:10.20944/preprints202101.0593.v1

ture describes the crystallization of the metal around a small hydrogen bubble that adheres to the surface. The hydrogen bubble can be formed during electrolysis because of residual water present in the bath from hydrated salts or from the surrounding air (the galvanic bath was not protected against contact with air here).

Based on the first results, subsequent experiments were focused on the process in baths with higher concentrations of copper acetate (> 35 mg/mL of CuAc) and at the favorable temperatures of 75°C and 100°C. These parameters allowed for obtaining uniform and compact coatings, especially in the range of current density from 3 to 12 mA·cm^{-2}. Some exemplary coatings with fine-grained structures are presented in Figures 3 and 4.

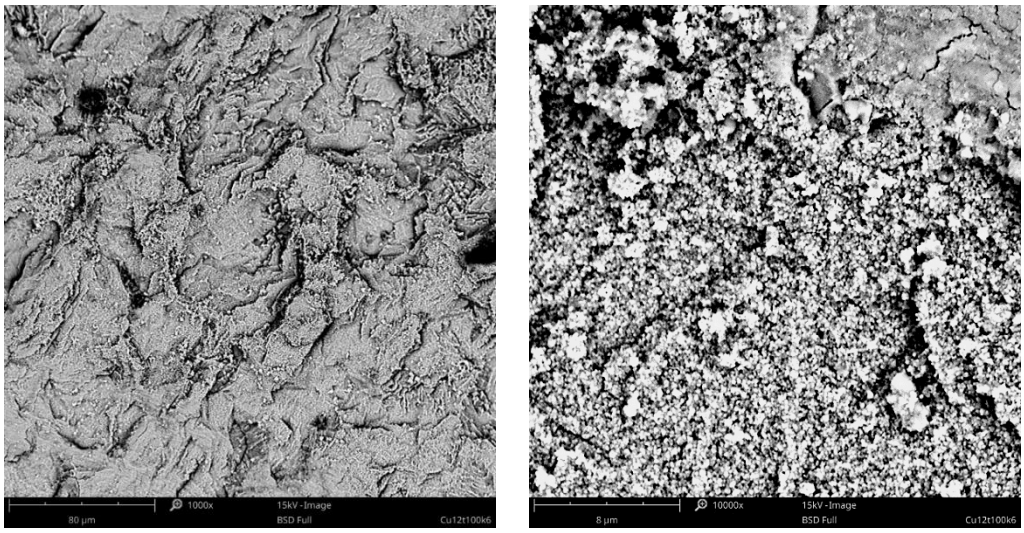

(**a**) (**b**)

Figure 3. SEM images of the Cu coating electrodeposited in the bath with 30 mg/mL of CuAc at a temperature of 100°C (j_c = 12 mA/cm^2, t = 7,5 min); Magnification: (**a**) x1000; (**b**) x 10000.

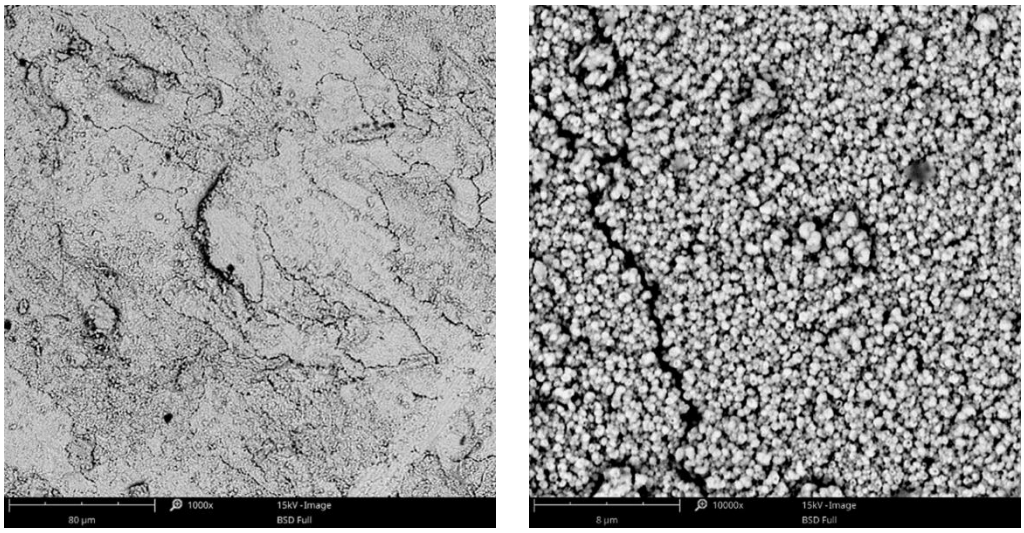

(**a**) (**b**)

Figure 4. SEM images of the Cu coating electrodeposited in the bath with 60 mg/mL of CuAc at a temperature of 75°C (j_c = 12 mA·cm^{-2}, t = 7,5 min); Magnification: (**a**) x1000; (**b**) x 10000.

3.1.2. Zinc coatings

Preprints (www.preprints.org) | NOT PEER-REVIEWED | Posted: 28 January 2021 doi:10.20944/preprints202101.0593.v1

In the case of the zinc electrodeposition, the formation of coatings was observed only from the baths with relatively high zinc acetate concentrations (> 430 mg/mL of ZnAc). Zinc coatings were not possible in the baths with lower concentrations. The coatings deposited from the bath containing 430 mg/mL of ZnAc had a characteristic, needle-shaped structure, and were not very tight nor compact (Figure 5). The coatings were also not homogeneous macroscopically. However, the increase of the zinc salt concentration to 600 g/dm^3 or 800 mg/mL ensured that the coatings were fine-grained as well as uniform, macro- and microscopically (Figure 6). The best quality of the zinc coatings was received at a cathodic current density in the range of 1.5–6.0 mA·cm^{-2}. When using a lower current density at the temperatures of 75°C and 100°C, the electrodeposition of zinc coatings was possible; a use of higher current density most often caused the formation of dull, poor quality coatings.

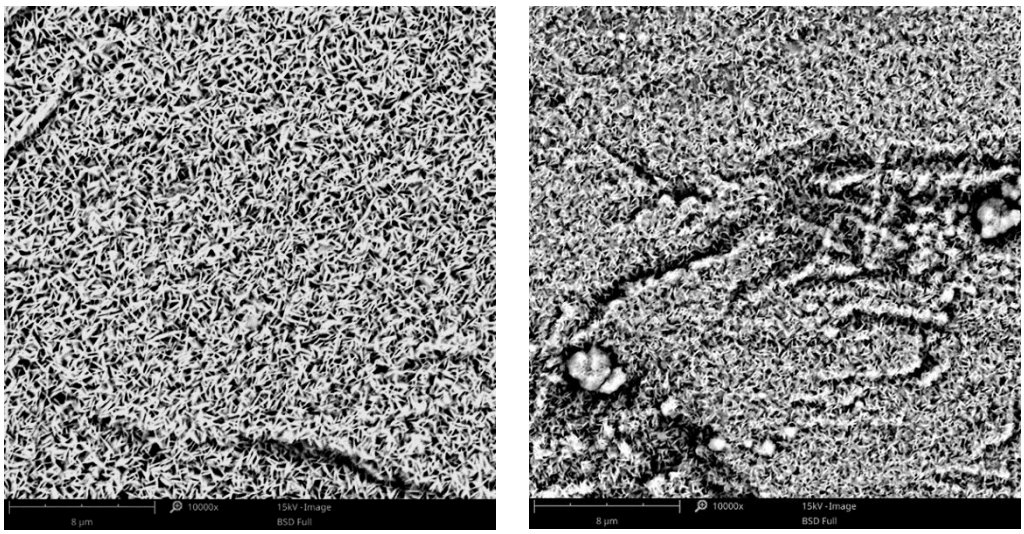

(**a**) (**b**)

Figure 5. SEM images of the Zn coating electrodeposited in the bath with 430 mg/mL of ZnAc at a temperature of: (**a**) 75°C (j_c = 3 mA·cm^{-2}, t = 15 min); (**b**) 100°C (j_c = 24 mA·cm^{-2}, t = 2 min).

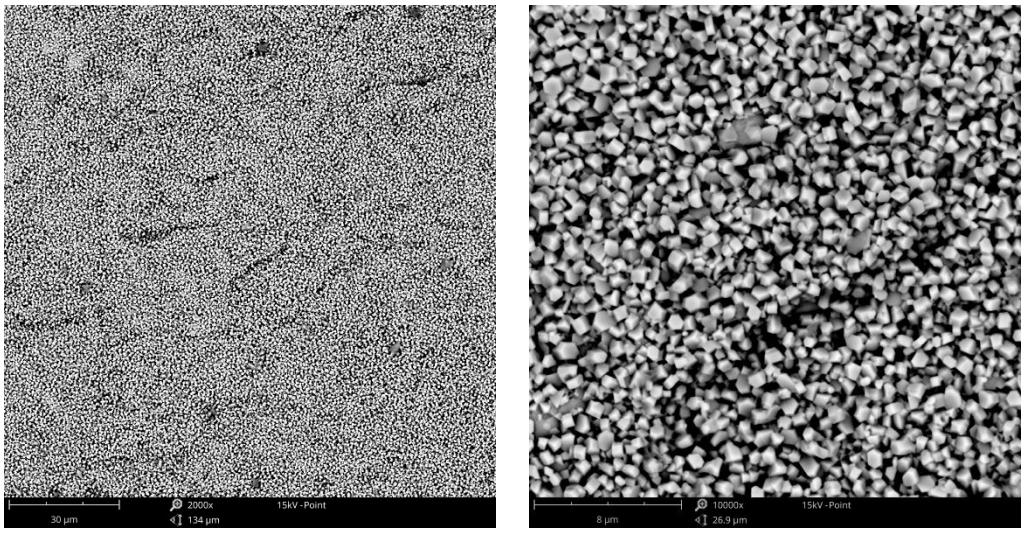

(**a**) (**b**)

Figure 6. SEM images of the Zn coating electrodeposited in the bath with 800 mg/mL of ZnAc at a temperature of 100°C (j_c = 3 mA·cm^{-2}, t = 15 min); Magnification: (**a**) x2000; (**b**) x10000.

3.1.3. Cu-Zn coatings

Preprints (www.preprints.org) | NOT PEER-REVIEWED | Posted: 28 January 2021 doi:10.20944/preprints202101.0593.v1

The use of baths with lower concentrations of zinc (CuZn-1 and CuZn2) resulted in the formation of homogeneous and porous coatings. The deposits obtained at low current densities had the characteristic olive-like structure (Figure 7a), similar to the one received in the case of the copper coating (Fig. 2b). Both coatings were electrodeposited at low current densities (0.75 and 1.5 mA·cm^{-2}), which suggests that in the process conditions, the low deposition rate favors the olive-like structure formation. The increase in the current density to 12 mA·cm^{-2} led to a change in the structure. The typical olive structures occurred less often and had a different characteristic porous structure (Figure 7b). In the case of the coatings electrodeposited in the baths with higher concentration of zinc (CuZn-3 and CuZn-4 baths), the structure was mainly fine-grained, similar to the copper coating (Fig. 4).

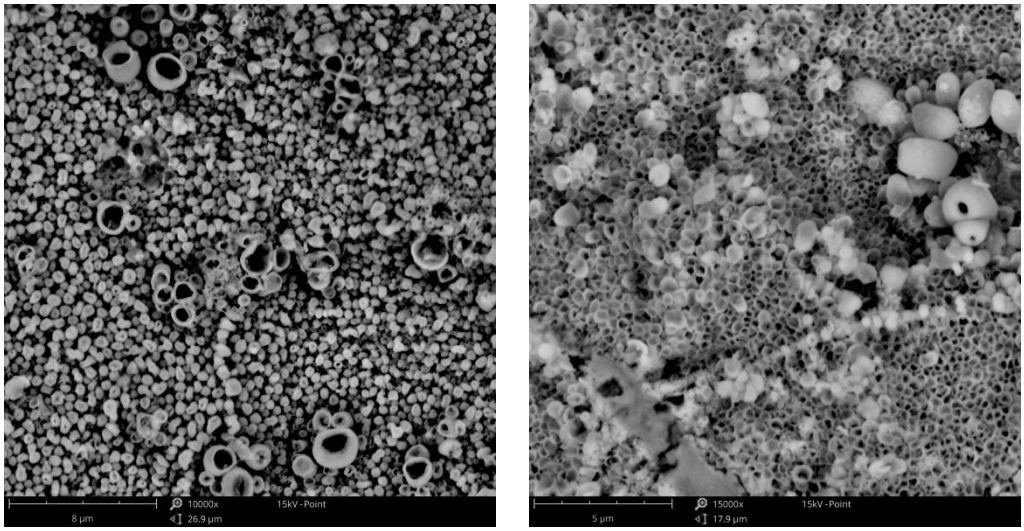

(**a**) (**b**)

Figure 7. SEM images of the Cu-Zn coating electrodeposited in the CuZn-1 bath at a temperature of 100°C, at a current density of: (**a**) j_c = 1.5 mA·cm^{-2} (magn. x10000; (**b**) j_c = 12 mA·cm^{-2} (magn. x15000)

3.2. Chemical composition of the Cu-Zn coatings

The chemical composition of the brass coatings was dependent on the bath composition as well as the current density. It was analyzed by two methods: EDX and ICP-OES. The exemplary EDX spectra, which show the significant influence of current density on the composition of the alloy, are presented in the Figure 8.

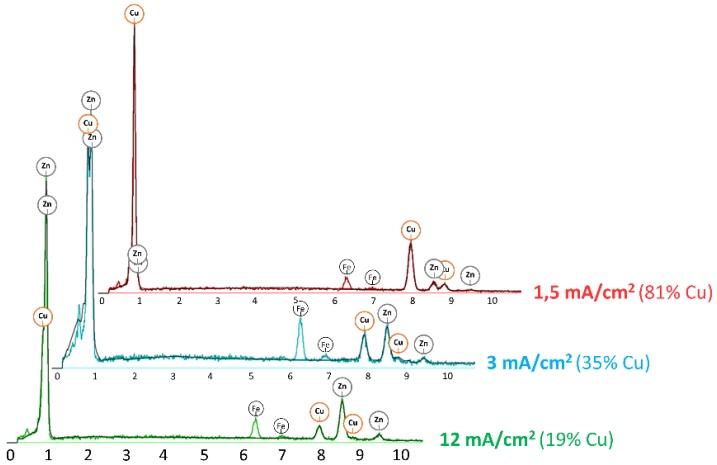

Figure 8. The EDS spectra of the brass coatings electrodeposited in the CuZn-4 bath (T = 100°C)

It was noted that in the case of all galvanic baths, the increase in current density caused a decrease in the amount of copper present in the alloy. Moreover, the concentration of zinc

Preprints (www.preprints.org) | NOT PEER-REVIEWED | Posted: 28 January 2021 doi:10.20944/preprints202101.0593.v1

acetate in the bath also had a strong influence on the alloy composition. The amount of zinc in the alloy increased with increasing amounts of ZnAc in the bath. The arrangement of the chemical composition of the received brass alloys is presented in Figure 9. The results obtained by ICP-OES are nearly identical to those obtained by EDX analysis; the differences were less than 2 at.%. The highest concentration of copper (96 at.%) was detected in the case of the alloy deposited in the CuZn-1 bath at a current density of 1.5 mA·cm^{-2} and the lowest percentage of copper (19 at.%) was detected from the alloy formed in the CuZn-4 bath at a current density of 12 mA·cm^{-2}. Therefore, the composition of the brass coatings may be relatively easily varied by two parameters (i.e., j_c and bath composition) over a wide range of chemical compositions of the alloy.

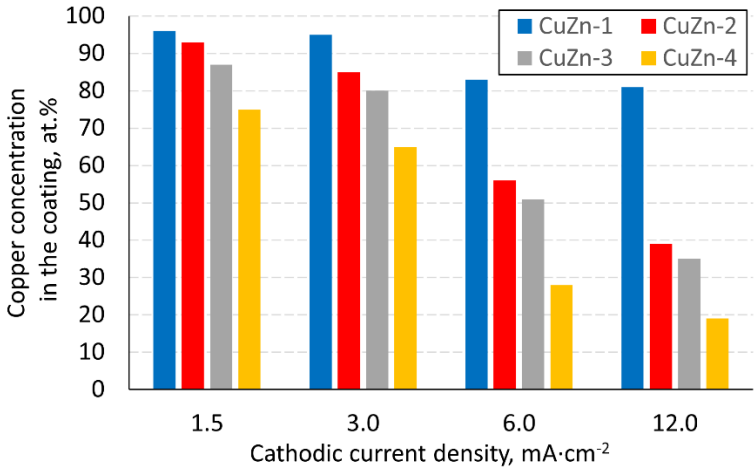

Figure 9. The bar chart showing chemical composition of the brass coatings (at.% of copper)

The correlation between chemical composition of the alloys and the galvanic baths which were used for their formation led to the classification of each specific type of electrodeposition. According to the Brenner's classification, in the studied range of parameters, the electrodeposition can be assigned as a normal type of codeposition. It means that copper, which is the more noble metal than zinc, deposits preferentially and the content of copper in the alloy is higher than in the plating solution. The correlation is presented in Figure 10.

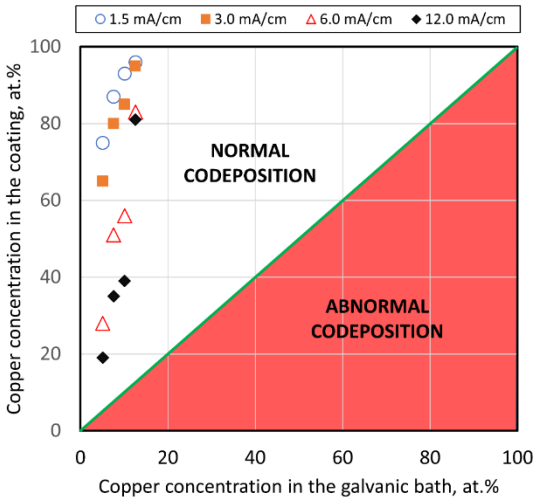

Figure 10. Graphical presentation of the influence of the galvanic bath composition and current density on the type of codeposition according to Brenner's classification (green line refers to regular codeposition)

Normal codeposition is also typical in the case of electrodeposition of brass coatings from cyanide baths, but it should be noted that abnormal codeposition with underpotential deposition of zinc is also possible [34].

Preprints (www.preprints.org) | NOT PEER-REVIEWED | Posted: 28 January 2021 doi:10.20944/preprints202101.0593.v1

3.3. Roughness of the olive-like brass structured coatings

Based on the 3D surface reconstructions, the characteristic parameters (R_a, R_z) for the brass coating with the olive-like structure as well as the fine-grained copper and zinc coatings were determined (Figure 11).

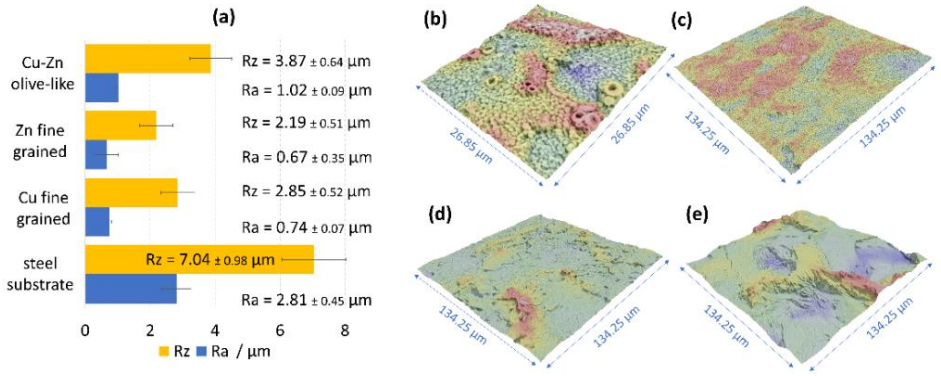

Figure 11. Roughness results (a) obtained on the basis of the 3D surface reconstructions of: **(b)** brass coating of olive-like structure; **(c)** fine-grained copper coating; **(d)** fine-grained zinc coating; **(e)** etched steel substrate.

Despite the high porosity of the brass coatings, the roughness of the coating was significantly lower than the roughness of the etched S235JR steel, which was a substrate in the process. The arithmetic roughness coefficient (R_a) for the steel was 2.85 ± 0.45 µm, whereas the R_a for the olive-like structured brass was 1.02 ± 0.45 µm. However, the fine-grained coatings of copper and zinc had much lower roughness: 0.76 ± 0.07 µm and 0.67 ± 0.07 µm, respectively. The results obtained for the three types of coatings showed that the acetate galvanic baths based on 1-ethyl-3-methylimidazolium acetate led to coatings with diminished surface roughnesses without the use of any additives.

3.4. Corrosion resistance of the coatings

Corrosion resistance studies were focused on the selected coatings, which were different chemical compositions and different structures. Moreover, the measurements were also done for the steel substrate to compare it to the coatings. The obtained potentiodynamic curves are presented in the Figure 12, and all parameters that defined the corrosion resistance were arranged in Table 3.

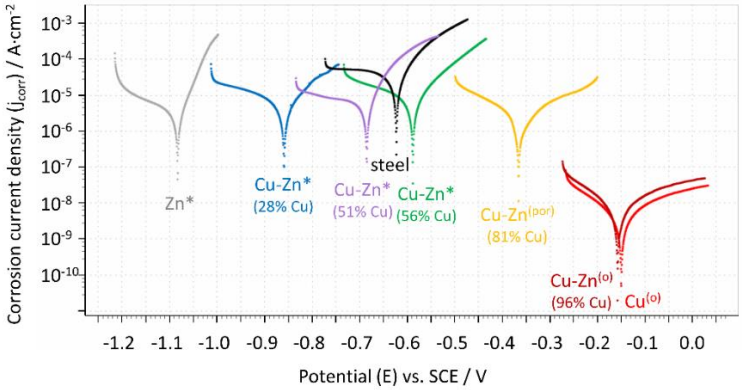

Figure 12. Potentionynamic curves for the steel substrate as well as for the selected coatings (Cu, Zn, Cu-Zn) with different structure: * – fine grained coatings; (por) – porous coating; (o) – coatings with olive-like structure.

Table 3. Summary of the results obtained by the Tafel potentiodynamic method.

Coating type	at.% of Cu in coating	Structure of coating	E_{corr} vs. SCE V	j_{corr} µA·cm^{-2}	R_p kΩ·cm^2

Preprints (www.preprints.org) | NOT PEER-REVIEWED | Posted: 28 January 2021 doi:10.20944/preprints202101.0593.v1

Cu	100	olive-like	-0.148	$3.1 \cdot 10^{-3}$	4726.8
Cu-Zn	96	olive-like	-0.156	$5.3 \cdot 10^{-3}$	4359.0
Cu-Zn	81	porous	-0.364	1.97	13.65
Cu-Zn	56	fine-grained	-0.587	6.50	3.67
Cu-Zn	51	fine-grained	-0.684	5.54	3.76
Cu-Zn	28	fine-grained	-0.858	5.48	4.58
Zn	0	fine-grained	-1.082	5.60	3,97
Steel (substrate)	-	-	-0.621	27.8	0.90

The highest value of corrosion potential was for the copper coating (E_{corr} = –0.148 V) and the lowest was for the zinc coating (E_{corr} = –1.082 V), which is in good accordance with their position in the electrochemical series of metals. The brass coatings had intermediate values of corrosion potential, which increased with the increase in copper concentration in the alloy. A similar relationship has been observed by El-Sherif et al. [35], who studied the electrochemical behavior of brasses with varied zinc percentages.

The worst corrosion resistance in the group of investigated materials was identified for the steel substrate, which was characterize by the highest corrosion current density (j_{corr} = 27.8 μA·cm^{-2}) and the lowest polarization resistance (R_p = 0.9 kΩ·cm^2). The values of corrosion potential as a part of the obtained coatings were lower than the E_{corr} value of the steel (E_{corr} = 0.621 V), meaning the coatings exhibited anodic character. There are zinc coatings and brass coatings with a relatively low percentage of the more noble metal (up to 51 at.% of copper). The copper coating as well as the brass coating with a concentration of copper above 56 at.% had higher a corrosion potential than steel, so they were cathodic type coatings in the chloride solution.

It was found that the structure of the studied coatings had very significant effects on the corrosion properties of the coating. All fine-grained coatings were characterized by good corrosion resistance, regardless of their composition. In this group of coatings, the corrosion current density values were between 5.6 and 6.5 μA·cm^{-2} and polarization resistance values were between 3.67 and 4.58 kΩ·cm^{-2}. The brass coating (81 at.% of Cu) with the porous structure, presented in Figure 7b, had slightly better anticorrosion properties (j_{corr} = 1.97 μA·cm^{-2}, R_p = 13.65 kΩ·cm^{-2}) than the fine-grained coatings. The results obtained for Cu and CuZn coatings with olive-like structures were surprising because the corrosion parameters (j_{corr}, R_p) were three orders of magnitude different than those of the fine-grained coatings, which indicates extremely high corrosion resistance. The most probable reason for the phenomenon is the stymied penetration of the corrosion medium into the inside part of the olive-like pores ensured by the very characteristic structure. After the immersion, the pores are still saturated by air and the corrosive solution has no direct contact with the surface of the porous coating. Moreover, the hypothesis could be lent credence by the fact that the improved porous coating (with 81 at% of Cu) has a mainly open-pore structure with some olive-like structure (lone olives, also noticeable in Figure 7b). A similar explanation which connects the improved corrosion resistance of porous materials with their structure has been presented by Seath et al. [36], who found that for unsintered porous titanium, the corrosion resistance increases with porosity.

5. Conclusions

- The galvanic baths based on 1-ethyl-3-methylimidazolium acetate ionic liquid allow for the electrodeposition of copper, zinc, and brass coatings;
- The structure of the obtained coatings is strongly dependent on the process parameters. The three main structures observed were fine-grained, porous and olive-like;
- The composition of the brass coatings could be varied by cathodic current density as well as bath composition over a wide range of chemical compositions of the alloy. The parameters led to alloys with 19–96 at.% copper;

- Brass electrodeposition occurs as a normal type of codeposition, according to Brenner's classification;
- The electrodeposited coatings were characterized by lower roughness than the steel substrate;
- All metallic and alloy coatings had good corrosion resistance, which were found to be dependent on their structure. Substantial improvement in corrosion properties was found in the case of copper and brass coatings with olive-like structures;
- The proposed procedure of electrodeposition allows for the formation of porous copper and brass coatings, which could serve as alternatives to other methods, e.g., powder sintering. Electrodeposition has the potential to be used in many applications such as for supports for catalysts and for the production of active electrodes for electrocatalysis. Moreover, the porous coatings may be modified by incorporating corrosion inhibitors or other substances in order to improve their functional properties.

Author Contributions: Conceptualization, A.M. and W.S.; methodology, A.M and N.Ł.; software, A.M. and N.Ł.; formal analysis, A.M and N.Ł.; investigation, A.M., N.Ł. and M.S.; data curation, A.M.; writing—original draft preparation, A.M.; writing—review and editing, A.M.; visualization, A.M.; supervision, W.S and M.S.; All authors have read and agreed to the published version of the manuscript.

Funding: Please add: This research received no external funding.

Institutional Review Board Statement: Not applicable.

Informed Consent Statement: Not applicable.

Data Availability Statement: Data is contained within the article.

Acknowledgments: We would like to thank Agata Jakóbik-Kolon for her support in the ICP studies.

Conflicts of Interest: The authors declare no conflict of interest. The funders had no role in the design of the study; in the collection, analyses, or interpretation of data; in the writing of the manuscript, or in the decision to publish the results.

References

1. Zhu, H.H.; Lu, L.; Fuh, J.Y. Development and characterisation of direct laser sintering Cu-based metal powder. *J. Mater. Process. Technol.* **203**, 140, 314–317.
2. Lesnikov, V.P.; Kuznetsov, V.P.; Goroshenko, Yu.O.; Rozhko, A.L. Diffusion saturation of nickel alloys with aluminum and chromium from the gas phase by the circulation method. *Met. Sci. Heat Treat.* **1998**, 40, 412–416.
3. Ryabchikov, A.I.; Sivin, D.O.; Bozhko, I.A.; Stephanov, I.B.; Shevelev, A.E. Microstructure of titanium alloy modified by high-intensity implantation of low and high-energy aluminium ions. *Surf. Coat. Technol.* **2020**, 391, 125722.
4. Gamburg, Y. D.; Zangari, G. Electrodeposition of alloys. In: *Theory and practice of metal electrodeposition*., 2011th ed.; Springer: New York, USA, 2011, pp. 205–232.
5. Musa, A.Y.; Slaiman, Q.J.M.; Kadhum, A.A.H.; Takriff, M. S. Effects of agitation, current density and cyanide concentration on Cu-Zn alloy electroplating. *Eur. J. Sci. Res.* **2008**, 22, 517–524.
6. Haciibrahimoglu, M.Y.; Yavuz, A.; Oztas, M.; Bedir, M. Electrochemical and structural study of Zn-rich brass deposited from py-rophosphate electrolyte onto the carbon steel. *Dig. J. Nanomater. Biostructures.* **2016,** 11, 251–262.
7. Vivegnis, S.; Krid, M.; Delhalle, J.; Mekhalif, Z.; Renner, F.U. Use of pyrophosphate and boric acid additives in the copper-zinc alloy electrodeposition and chemical dealloying. *J. Electroanal. Chem.* **2019**, 848, 113310.
8. Silva, F.L.G.; do Lago, D.C.B.; Delia, E.; Senna, L.F. Electrodeposition of Cu-Zn alloy coating from citrate baths containing benzotriazole and cysteine as additives. J. Appl. Electrochem. **2010**, 40, 2013–2022.
9. Tintelecan, M.; Iluțiu-Varvara, D.A.; Alabanda, O.R.; Sas-Boca, I.M. A technical version of achieving a brass coated surface on steel wires. *Procedia Manuf.* **2020**, 46, 12–18.
10. Rossi, A. A tartrate-based alloy bath for brass plated steel wire production. *J. Appl. Electrochem.* **1992**, 22, 64–72.
11. Barros, K.S.; Ortega, E.M.; Pérez-Herranz, V.; Espinosa, D.C.R. Evaluation of brass electrodeposition at RDE from cyanide-free bath using EDTA as a complexing agent. *J. Electroanal. Chem.* **2020**, 865, 1141.
12. Ramírez, C.; Calderón, J.A. Study of the effect of triethanolamine as a chelating agent in the simultaneous electrodeposition of copper and zinc from non-cyanide electrolytes. *J. Electroanal. Chem.* **2016**, 765, 132–139.
13. Ibrahim, M.A.M.; Bakdash, R.S. New cyanide-free ammonia bath for brass alloy coatings on steel substrate by electrodeposition. *Inter. J. Electrochem. Sci.* **2015**, 10, 9666–9677.

14. Fujiwara, Y.; Enomoto, H. Electrodeposition of Cu–Zn alloys from glucoheptonate baths. *Surf. Coat. Technol.* **1988**, 35, 101–111.
15. Ibrahim, M.A.M.; Bakdash, R.S. Copper-rich Cu–Zn alloy coatings prepared by electrodeposition from glutamate complex electrolyte: Morphology, structure, microhardness and electrochemical studies. *Surf. Interfaces.* **2020**, 18, 100404.
16. Rashwan, S.M. Electrodeposition of Zn–Cu coatings from alkaline sulphate bath containing glycine. *Trans. Inst. Met. Finish.* **2007**, 85, 217–224.
17. Ghorbani, M.; Mazaheria, M.; Khangholi K.; Kharazi, Y. Electrodeposition of graphite-brass composite coatings and characterization of the tribological properties. *Surf. Coat. Technol.* **2001**, 148, 71–76.
18. Das, S.; Jena, S.; Banthia, S.; Mitra, A.; Das, S.; Das, K. Novel pulse potentiostatic electrodeposition route for obtaining pure intermetallic Cu5Zn8-CuZn composite coating using glycerol-NaOH based electrolyte with advanced scratch resistance and anti-corrosive properties. *J. Alloys Compd.* **2019**, 792, 770–779.
19. Freemantle, M. *An introduction to ionic liquids*, 1st ed.; Royal Society of Chemistry, Cambridge, UK, 2010; pp. 1–18.
20. Endres, F.; Abbott, A.P.; MacFarlane, D.R.; *Electrodeposition from ionic liquids*, 1st ed.; Wiley-VCH: Weinheim, Germany, 2008; pp. 1–13.
21. Haerens, K.; Matthijs, E.; Chmielarz, A.; Van der Bruggen, B. The use of ionic liquids based on choline chloride for metal deposition: a green alternative? *J. Environ. Manage.* **2009**, 90, 3245–3252.
22. Cao, X.; Xu, L.; Shi, Y.; Wang, Y.; Xue, X. Electrochemical behavior and electrodeposition of cobalt from choline chloride-urea deep eutectic solvent. *Electrochim. Acta.* **2019**, 295, 550–557.
23. Wang, J. et al. Low temperature electrochemical deposition of aluminum in organic bases/thiourea-based deep eutectic solvents. *ACS Sustain. Chem. Eng.* **2018**, 6, 15480–15486.
24. Alesary, H.F. et al. Effects of additives on the electrodeposition of Zn-Sn alloys from choline chloride/ethylene glycol-based deep eutectic solvent. *J. Electroanal. Chem.* **2020**, 874, 114517.
25. Li, M.; Wang, Z.; Reddy, R.G.; Cobalt electrodeposition using urea and choline chloride. *Electrochim. Acta.* **2014**, 123, 325-331
26. Xie, X.; Zou, X.; Lu, X.; Lu, C.; Cheng, H.; Xu, Q.; Zhou, Z. Electrodeposition of Zn and Cu–Zn alloy from ZnO/CuO precursors in deep eutectic solvent. *Appl. Surf. Sci.* **2016**, 386, 481–489.
27. Rousse, C.; Beaufils, S.; Fricoteaux, P. Electrodeposition of Cu–Zn thin films from room temperature ionic liquid. *Electrochim. Acta.* **2013**, 107, 624–631.
28. Zhang, J.; Ma, X.; Zhang, J.; Yang, P.; An, M.; Li, Q. Electrodeposition of Cu-Zn alloy from EMImTfO ionic liquid/ethanol mixtures for replacing the cyanide zincate layer on Al alloy, *J. Alloys Compd.* **2019**, 806, 79–88.
29. Guo, L.; Oskam, G.; Radisic, A.; Hoffman, P.M.; Searson, P.C. Island growth in electrodeposition, *J. Phys D: Appl. Phys.* **2011**, 44, 443001.
30. Rokosz, K. et al. Characterization of porous phosphate coatings enriched with calcium, magnesium, zinc and copper created on CP titanium Grade 2 by plasma electrolytic oxidation. *Metals.* **2018**, 8, 411.
31. Rokosz, K.; Hryniewicz, T.; Pietrzak, K.; Dudek, Ł. Porous PEO coatings on titanium, obtained under DC regime, enriched in magnesium, calcium, zinc, and copper. *World Sci. News*. **2018**, 94, 99–114.
32. Komarova, E.G.; Kazantseva, E.A.; Chaikina, M.V.; Bulina, N.V.; Sedelnikova, M.B.; Sharkeev, Y.P. Morphological and structural features of micro-arc Zn-Si-containing calcium phosphate coatings. *Mater. Today.* **2020**, 25, 439–442.
33. Brenner, A. *Electrodeposition of alloys*, 1st ed.; Academic Press Inc.: New York/London, USA/UK, 1963.
34. Fujiwara, Y.; Enomoto, H. Electrodeposition of β′-brass from cyanide baths with accumulative underpotential deposition of Zn. *J. Electrochem. Soc.* **2000**, 147, 1840–1846.
35. El-Sherif, R.M.; Ismail, K.M.; Badawy, W.A. Effect of Zn and Pb as alloying elements on the electrochemical behavior of brass in NaCl solutions. *Electrochim. Acta*. **2004**, 49, 5139–5150.
36. Seah, K.H.W; Thampuran, R.; Chen, X.; Teoh, S.H. A comparison between the corrosion behaviour of sintered and unsintered porous titanium. *Corr. Sci.* **1995**, 37, 1333–1340.